Regional-scale lateral carbon transport and CO_2 evasion in temperate stream catchments

Katrin Magin[1], Celia Somlai-Haase[1], Ralf B. Schäfer[1] and Andreas Lorke[1]

[1]Institute for Environmental Sciences, University of Koblenz-Landau, Fortstr. 7, D-76829 Landau, Germany

Correspondence to: Katrin Magin (magi6618@uni-landau.de)

Abstract. Inland waters play an important role in regional to global scale carbon cycling by transporting, processing and emitting substantial amounts of carbon, which originate mainly from their catchments. In this study, we analyzed the relationship between terrestrial net primary production (NPP) and the rate at which carbon is exported from the catchments in a temperate stream network. The analysis included more than 200 catchment areas in southwest Germany, ranging in size from 0.8 to 889 km^2 for which CO_2 evasion from stream surfaces and downstream transport with stream discharge were estimated from water quality monitoring data, while NPP in the catchments was obtained from a global data set based on remote sensing. We found that on average 2.7 % of terrestrial NPP (13.9 g C m^{-2} yr^{-1}) are exported from the catchments by streams and rivers, in which both CO_2 evasion and downstream transport contributed about equally to this flux. The average carbon fluxes in the catchments of the study area resembled global and large-scale zonal mean values in many respects, including NPP, stream evasion as well as the carbon export per catchment area in the fluvial network. A review of existing studies on aquatic-terrestrial coupling in the carbon cycle suggests that the carbon export per catchment area varies in a relatively narrow range, despite a broad range of different spatial scales and hydrological characteristics of the study regions.

Keywords

Regional carbon cycle, terrestrial-aquatic coupling, net primary production, CO_2 degassing from streams, land use

1 Introduction

Inland waters represent an important component of the global carbon cycle by transporting, storing and processing significant amounts of organic and inorganic carbon (C) and by emitting substantial amounts of carbon dioxide (CO_2) to the atmosphere (Cole et al., 2007;Aufdenkampe et al., 2011). Globally about 0.32 to 0.8 Pg C is emitted per year as CO_2 from lakes and reservoirs (Raymond et al., 2013;Barros et al., 2011). For streams and rivers the global estimates range from 0.35 to 1.8 Pg C yr^{-1} (Raymond et al., 2013;Cole et al., 2007), where the lower estimates can be considered as conservative because they omit CO_2 emissions from small headwater streams. In 2015 global CO_2 evasion from rivers and streams was estimated at 0.65 Pg C yr^{-1} (Lauerwald et al., 2015). Comparable amounts of carbon are discharged into the oceans by the world's rivers (0.9 Pg C yr^{-1}) and stored in aquatic sediments (0.6 Pg C yr^{-1}) (Tranvik et al., 2009). In total, evasion, discharge and storage of C in inland waters have been estimated to account for about 4 % of global terrestrial net primary production (NPP) (Raymond et al., 2013) or 50-70 % of the total terrestrial net ecosystem production (NEP) (Cole et al., 2007). A recent continental-scale analysis, which combined terrestrial productivity estimates from a suite of biogeochemical models with estimates of the total aquatic C yield for the conterminous United States (Butman et al., 2015), resulted in mean C export rates from terrestrial into freshwater systems of 4 % of NPP and 27 % of NEP. These estimates varied by a factor of four across 18 hydrological units with surface areas between 10^5 and 10^6 km^2.

The substantial lateral and vertical transport of terrestrial-derived C in inland waters is currently not accounted for in most bottom-up estimates of the terrestrial uptake rate of atmospheric CO_2 (Battin et al., 2009) and results in high uncertainties in regional-scale C budgets and predictions of their response to climate change, land use and water management. Only few studies have quantified C fluxes and pools including inland waters at the regional-scale ($O(10^3\text{-}10^4$ $km^2)$) (Christensen et al., 2007;Buffam et al., 2011;Jonsson et al., 2007;Maberly et al., 2013) or for small (O(1-10 km^2)) catchments (Leach et al., 2016;Shibata et al., 2005;Billett et al., 2004). The majority of existing regional-scale studies on terrestrial-aquatic C fluxes are from the boreal zone and are characterized by a relatively large fractional surface area covered by inland waters, a high abundance of lakes and high fluvial loads of dissolved organic carbon (DOC). Landscapes in the temperate zone can differ in all these aspects, potentially resulting in differences in the relative importance of aquatic C-fluxes and flux paths (storage, evasion and discharge) in regional-scale C budgets. In this study, we analyzed the relationship between terrestrial NPP and CO_2 evasion and C discharge for more than 200 catchments in southwest Germany. The stream-dominated catchments range in size from 0.8 to 889 km^2 and are characterized by a relatively small fraction of surface water coverage (< 0.5 % of the land surface area). In contrast to studies from the boreal zone, the fluvial C load is dominated by dissolved inorganic carbon (DIC). Estimates of aquatic C export from the catchments were obtained from water quality and hydrological monitoring data and were related to terrestrial NPP derived from MODIS satellite data. The scale dependence of aquatic carbon fluxes in relation to NPP is analyzed by grouping the data according to Strahler stream order (Strahler, 1957). By comparing our results to a variety of published studies, we finally discuss the magnitude as well as the relative importance of different fluvial flux paths in regional-scale C budgets in different landscapes and climatic zones.

2 Materials and Methods

2.1 Study area and hydrological characteristics

The study area encompasses large parts of the federal state of Rhineland-Palatinate (RLP) in southwest Germany (Fig. 1). The average altitude is 323 m (48 m - 803 m) and the mean annual temperature and precipitation varied between 5.8 and 12.2 °C and 244 and 1576 mm during the time period between 1991 and 2011 at the 37 meteorological stations operated by the state RLP (http://www.wetter.rlp.de/). The dominating land cover in the study area is woodland (41 %, mainly mixed and broad-leaved forest), tilled land (37 %, mainly arable land and vineyards) and grassland (13 %, mainly pastures) (Corine land cover (EEA, 2006)). The fraction of peatland in the study area is small (0.95 km^2; 0.009% of the study area). 16 % of the study area contain carbonate bedrock.

Most of the rivers in RLP are part of the catchment area of the Rhine River. Other large rivers in the state are Mosel, Lahn, Saar and Nahe. The upland regions of RLP are sources to many small, steep and highly turbulent streams with gravel beds (MULEWF, 2015). Lakes in RLP are small with a total area of approximately 40 km^2 (Statistisches Landesamt Rheinland-Pfalz, 2014) and were omitted from the analysis. The river network has a total length of 15800 km and consists of stream orders (Strahler, 1957) between 1 and 7. A catchment map of RLP, consisting of subcatchments of 7729 river segments was provided by the state ministry (MULEWF, 2013), where a river segment refers to the section between a source and the first junction with another river or between two junctions with other rivers. All subsequent analyses were conducted separately for each stream order and streams of Strahler order >4 were omitted from the analysis because of the limited sample size with only few catchments available. Moreover, we omitted streams for which parts of the catchment area were outside of the study area. Overall, 3377, 1619, 861 and 453 stream segments were retained for the analysis for Strahler order 1 to 4, respectively. Annual mean discharge and length of the river segments were obtained from digital maps provided by the state ministry (MULEWF, 2013).

2.2 Aquatic carbon concentrations

DIC concentrations and partial pressure of dissolved CO_2 (pCO_2) in stream water were estimated from governmental water quality monitoring data which were acquired according to DIN EN ISO norms (DIN EN ISO 10523:2012-04;DIN EN ISO 9963-1:1996-02;DIN EN ISO 9963-2:1996-02).. The data include measurements of alkalinity, pH and temperature which were conducted between 1977 and 2011 (MULEWF, 2013). Sampling intervals differed between the sites and water sampling was conducted irregularly with respect to year and season. To exclude a potential bias resulting from the seasonality of DIC concentrations on the analysis, we only considered river segments for which at least one measurement was available for each season (spring, summer, autumn, winter). From these measurements, pCO_2 and DIC concentrations were estimated using chemical equilibrium calculations with the software PHREEQC (Version 2) (Parkhurst and Appelo, 1999). For 201 river segments with seasonally resolved measurements, we first computed seasonal mean pCO_2 and DIC concentrations, which subsequently were aggregated to annual mean values averaged over the entire sampling period:

$$\overline{pCO_{2_{annual}}} = (\overline{pCO_{2_{spring}}} + \overline{pCO_{2_{summer}}} + \overline{pCO_{2_{autumn}}} + \overline{pCO_{2_{winter}}})/4 \quad (1)$$

Measurements of dissolved and total organic C (DOC, TOC) were available only for 64 of these sampling sites.

2.3 Estimation of lateral DIC export and catchment-scale CO_2 evasion

The lateral export of DIC and the total CO_2 evasion from the upstream located stream network was calculated for each of the 201 sampling sites with seasonally averaged concentration estimates. Lateral DIC export from the corresponding catchments was calculated as the product of the mean DIC concentration and discharge. CO_2 evasion from the stream network upstream of each sampling site was estimated by interpolating pCO_2 for all river segments without direct measurements by averaging the mean concentrations by stream order and assigning them to all stream segments of the river network (Butman and Raymond, 2011). Stream width (w, in m), depth (d, in m) and flow velocity (v, in m s^{-1}) were estimated from the discharge (Q, in m^3 s^{-1}) using the following empirical equations (Leopold and Maddock Jr, 1953):

$$w = a * Q^b \qquad d = c * Q^d \qquad v = e * Q^f, \quad (2)$$

For the hydraulic geometry exponents and coefficients, the values from Raymond et al. (2012) were used (b=0.42, d=0.29, f=0.29, a=12.88, c=0.4 and e=0.19).

The water surface area (A, in m^2) was calculated as the product of length and width of the river segments. The average slope for each segment was estimated from a Digital Elevation Map (resolution 10 m) provided by the federal state of Rhineland-Palatinate (LVermGeoRP, 2012). Zhang and Montgomery (1994) investigated the effect of digital elevation model (DEM) resolution on slope calculation and performance in hydrological models for spatial resolutions between 2 and 90 m. They found that while a 10-m grid is a significant improvement over 30 m or coarser grid sizes, finer grid sizes provide relatively little additional resolution. Thus a 10-m grid size represents a reasonable tradeoff between increasing spatial resolution and data handling requirements for modeling surface processes in many landscapes. The gas transfer velocity of CO_2 at 20°C (k_{600}, in m d^{-1}) was calculated from slope (S) and flow velocity (v, in m s^{-1}) (Raymond et al., 2012).

$$k_{600} = S * v * 2841.6 + 2.03 \quad (3)$$

This gas transfer velocity was adjusted to the in situ temperature (k_T, in m d^{-1}) using the following equation:

$$k_T = k_{600} * \left(\frac{Sc_T}{600}\right)^{-0.5}, \quad (4)$$

where Sc_T is the Schmidt number (ratio of the kinematic viscosity of water and the diffusion coefficient of dissolved CO_2) at the in situ temperature (Raymond et al., 2012). Finally the CO_2 flux (F_D, in g C m^{-2} yr^{-1}) for each stream segment was calculated as:

$$F_D = k_T \cdot K_H\left(pCO_2 - pCO_{2,a}\right) \cdot M_C \quad (5)$$

The partial pressure of CO_2 in the atmosphere ($pCO_{2,a}$) was considered as constant (390 ppm) and the Henry coefficient of CO_2 at in-situ temperature (K_H in mol l^{-1} atm^{-1}) was estimated using the relationship provided in (Stumm and Morgan, 1996). M_C is the molar mass of C (12 g mol^{-1}). Finally, the total CO_2 evasion was estimated by

summing up the product of F_D with the corresponding water surface area for all stream segments located upstream of each individual sampling point.

2.4 Estimation of the catchment NPP

Average NPP in the catchment areas of the study sites were obtained from a global data set derived from moderate resolution imaging spectroradiometer (MODIS) observations of the earth observing system (EOS) satellites, which is available for the time period 2000 to 2013 with a spatial resolution of 30 arc seconds (~ 1 km^2) (Zhao et al., 2005). In this data set, NPP was estimated based on remote sensing observations of spectral reflectance, land cover and surface meteorology as described in detail by Running et al. (2004). We used mean NPP data (2000-2013) averaged over the catchment areas of the individual sampling sites.

2.5 Statistical analysis

Linear regressions (F-test) were used to analyze the data. Group differences or correlations with $p<0.05$ were considered statistically significant. For the regression of total aquatic C export rate and annual catchment NPP, data were log-transformed to correct for normal distribution. All statistical analyses were performed with R (R Development Core Team, 2011).

3 Results

3.1 Catchment characteristics and aquatic C load

The size of the analyzed catchment areas varied over three orders of magnitude (0.8 to 889 km^2) and the mean size increased from 9 km^2 for 1st order streams to 243 km^2 for streams of the order 4 (Table 1). Mean discharge and catchment area were linearly correlated (r^2=0.74, $p<0.001$). The runoff depth, i.e. the stream discharge divided by the catchment area, was relatively constant across stream orders with a mean value of 0.28 m y^{-1}, corresponding to 35 % of the annual mean precipitation rate in the study area. The mean discharge increased more than 30-fold from 0.06 to 2.2 m^3 s^{-1} for 1st to 4th order streams, respectively. Similarly, the estimated water surface area increased with increasing stream order from 0.24 to 0.42 % of the corresponding catchment size (Table 1).

Individual estimates of the CO_2 partial pressure at the sampling sites varied between 145 and 7759 ppm. Only 1 % of the pCO_2 values were below the mean atmospheric value (390 ppm), indicating that the majority of the stream network was a source of atmospheric CO_2 at all seasons. The pCO_2 was higher in summer (mean±sd: 2780±2098 ppm) and autumn (mean±sd: 2848±2019 ppm) than in winter (mean±sd: 2287±1716 ppm) and spring (mean±sd: 2172±2343 ppm). The total mean value of pCO_2 was 2083 ppm and pCO_2 and DIC did not differ significantly among the different stream orders (pCO_2: p=0.35; DIC: p=0.56). On average, DIC in the stream water was composed of 91.2 % bicarbonate, 0.4 % carbonate and 8.4 % CO_2.

The few available samples of DOC and TOC indicate that the organic C concentration was about one order of magnitude smaller than the inorganic C concentration (Table 1). There were no pronounced regional or temporal differences of organic carbon. Only a small fraction of TOC was in particulate form (on average 8.6 %) and TOC was linearly related to DIC, indicating that the organic load made up only 4 % of the total carbon load at the sampling sites (Fig. 2). The data are provided as supplementary material.

3.2 Catchment NPP and C budget

NPP increased linearly with catchment size (r^2=0.98, p<0.001), but the specific NPP, i.e. the total NPP within a catchment divided by catchment area, did not differ significantly (p=0.24) among catchments of different stream orders. The smallest mean value and the largest variability of specific NPP (mean±sd: 466±127 g C m^{-2} yr^{-1}, range: 106 to 661 g C m^{-2} yr^{-1}) was observed among the small catchments of 1st order streams, while the variability was consistently smaller for higher stream orders (Table 2). The total average of terrestrial NPP in the study area was 515±79 g C m^{-2} yr^{-1} (mean±sd).

In a simplified catchment-scale C balance, we consider the sum of the DIC discharge (DIC concentration multiplied by discharge) measured at each sampling site and the total CO_2 evasion from the upstream located stream network as the total amount of C that is exported from the catchment area through the aquatic conduit. The total evasion was estimated by interpolation with stream-order specific pCO_2 values assigned to the complete stream network. Given the small number of available measurements, we neglect the fraction of organic C which is exported with stream discharge. As demonstrated above, TOC load is small in comparison to the DIC load (Fig. 2), resulting in a comparably small (< 4 %) error.

The resulting CO_2 evasion rates decreased slightly, but not significantly (p=0.26) for increasing stream orders with a total mean evasion rate of 2032 g C m^{-2} yr^{-1} (expressed as per unit water surface area) (Table 2). The total aquatic evasion rate within catchments normalized by the size of the catchment increased significantly with stream order with a mean value of 6.6 g C m^{-2} yr^{-1}. (Table 2).

The total aquatic C export rate, i.e. the sum of evasion and DIC discharge, was strongly correlated with annual mean NPP averaged over the corresponding catchment area. Linear regression of the log-transformed data results in a power-law exponent of 1.06, indicating a nearly linear relationship (Fig. 3). As small streams of low stream order can be directly influenced by local peculiarities, the relationship is more variable for streams of Strahler order 1 and 2, while larger streams represent more average conditions over larger spatial scales with less variability. Most of the correlation between the total aquatic C export rate and the annual mean NPP, however, can be attributed to their common linear scale-dependence.

After normalization with catchment area, the total aquatic C export rate increased slightly with stream order (Fig. 4a). Also the fraction of NPP which was exported through the aquatic network, i.e. the sum of evasion and discharge, increased slightly, though not significantly (p=0.32), from 2.18 % for first-order stream to 2.72 % for

stream order 4 (Fig. 4b). This increase was related to increasing rates of CO_2 evasion in streams of higher order and the contribution of evasion to the total C export rate increased from 39 to 53 % (Fig. 4c). The increasing evasion is mainly caused by the increasing fractional water surface area for increasing stream orders (Table 1), because the CO_2 fluxes per water surface showed a rather opposing trend with decreasing fluxes for increasing stream orders (Table 2). On average 1.31 % of the catchment NPP are emitted as CO_2 from the stream network and 1.49 % are discharged downstream (Table 2).

No regional (large-scale) pattern or gradients were observed in the spatial variation of catchment-scale NPP and aquatic C export (Fig. 5).

4 Discussion

4.1 Uncertainty analysis

Our estimates are subject to a number of uncertainties associated with sampling and interpolation and systematic errors including the neglect of carbon burial in sediments, carbon export and evasion as methane and unresolved spatial and temporal variability.

According to Abril et al. (2015), high uncertainties of pCO_2 estimates from pH and alkalinity measurements occur at pH values <7. In our study, only 7 % of the pH values were <7. For pH>7 the median and mean relative errors are 1% and 15%, respectively (Abril et al., 2015). Raymond et al. (2013) estimated uncertainties from comparisons of estimates obtained using approaches comparable to the present study with direct measurements of CO_2 concentration on streams. For a density of sampling locations of 0.02 sites per km^2 (corresponding to this study) they derived an uncertainty of 30 %. Similarly, Butman and Raymond (2011) estimated uncertainties of overall flux estimates of 33 %, based on Monte Carlo simulation of similar data for hydrographic units in the United States.

While the riverine carbon concentrations were obtained from measurements that covered a time period from 1977 to 2011, the NPP data were available for the time period from 2000 to 2013. In boreal and subtropical rivers a decadal increasing DIC export due to the climate change and anthropogenic activities has been observed (Walvoord and Striegl, 2007;Raymond et al., 2008), therefore the different time periods covered by the two data sets might pose a problem. Comparisons of DIC measurements in the study area between 1977-1999 and 2000-2011 however did not show significant changes. Furthermore, the sampling frequency for DIC increased so that the majority of DIC measurements originated from the same time period as the NPP data (Supplementary Material).

The hydraulic geometry exponents and coefficients used in this study were derived from various data sets obtained in North America, not for central Europe. Unfortunately, we are not aware of a comparably extensive data set of hydraulic geometry data derived for European rivers. The coefficients have been applied in global studies before, e.g. Raymond et al. (2013). A comparison of hydraulic geometry coefficients derived from various data sets, including data from England, Australia and New Zealand, is presented in Butman and Raymond (2011), who

estimated that the error associated with uncertainties of hydraulic geometry coefficients is rather small, compared to uncertainties derived for C-fluxes.

Carbon burial in sediments was neglected in this study but can make a significant contribution to catchment-scale C balances. Estimates vary between 22 % at a global scale (Aufdenkampe et al., 2011), 14 % for the Conterminous U.S. (Butman et al., 2015) and 39% for the Yellow River network (Ran et al., 2015). However, C storage in aquatic systems occurs mainly in lakes and reservoirs, which are virtually absent in the study area. Therefore we consider the bias caused by neglecting storage to be small in comparison to remaining uncertainties (30%).

Similarly, the transport of carbon as methane was neglected because measurements of methane concentration or fluxes were not available for the study area. According to a recent meta-analysis, the dissolved methane concentration in headwater streams varies mainly between 0.1 and 1 µmol L^{-1}, with streams in temperate forests being at the lower end (Stanley et al., 2016). As the methane makes up only a small fraction of total carbon in comparison to the mean DIC concentration in the present study (500 µmol L-1), it can be assumed that methane makes a rather small contribution to the catchment scale carbon balance.

Since no time-resolved discharge data were available for the sampling sites we cannot account for extreme events. Moreover, no information were available if the governmental monitoring included sampling during floods. Given the stochastic nature and short duration, we expect that such samples are at least underrepresented. Since it has been observed that high-discharge events can make a disproportionally high contribution to annual mean carbon export from catchments, we consider our estimates as a lower bound.

4. 2. An average study region

The average carbon fluxes in the catchments of the study area resemble global and large-scale zonal mean estimates in many aspects. The mean atmospheric flux of CO_2 from the stream network of 2031±1527 g C m^{-2} yr^{-1} is in close agreement with bulk estimates for streams and rivers in the temperate zone of 2630 (Aufdenkampe et al., 2011) and 2370 g C m^{-2} yr^{-1} (Butman and Raymond, 2011). The fractional surface coverage of streams and rivers (0.42 % for stream order 4) corresponds to the global average of 0.47 % (Raymond et al., 2013) and also mean terrestrial NPP in the catchments (515 g C m^{-2} yr^{-1}) was in close correspondence to recent global mean estimates (495 g C m^{-2} yr^{-1} (Zhao et al., 2005)).

By combining CO_2 evasion and downstream C-export by stream discharge, we estimated that 2.7 % of terrestrial NPP (13.9 g C m^{-2} yr^{-1}) are exported from the catchments by streams and rivers, in which both evasion and discharge contributed equally to this flux. Also these findings are in close agreement with global and continental scale estimates, of 16 and 13.5 g C m^{-2} yr^{-1}, respectively (Table 3).

4.3. Aquatic C export across spatial scales

Though not exhaustive, Table 3 provides data from a large share of existing studies relating the aquatic C export to terrestrial production in the corresponding catchments which cover a broad range of spatial scales and different landscapes. Except for the tropical forest of the Amazon basin, the aquatic carbon export normalized to catchment

area estimated for temperate streams in our study, is surprisingly similar to those estimated at comparable and at larger spatial scale. In the Amazon, the fraction of terrestrial production that is exported by the fluvial network is more than twofold higher (nearly 7 % of NPP (Richey et al., 2002)). However, that a large fraction of the regional NPP in the Amazon is supported by aquatic primary production by macrophytes and carbon export is predominantly controlled by wetland connectivity, with wetlands covering up to 14 % of the land surface area (Abril et al., 2013). An additional peculiarity of the Amazon is, that in contrast to the remaining systems, the vast majority (87 %) of the total C export is governed by CO_2 evasion (Table 3), whereas lateral export constitutes a much smaller component. An exceptionally low fraction of NPP that is exported from aquatic systems at larger scale was estimated for the English Lake District (1.6 % (Maberly et al., 2013)), though only CO_2 evasion from lake surfaces was considered, i.e. downstream discharge by rivers was ignored. Their estimate agrees reasonably well with the fraction of catchment NPP that was emitted to the atmosphere from the stream network in the present study (1.3 %). If a similar share of catchment NPP was exported with river discharge also in the Lake District, the average mass of C exported from the aquatic systems per unit catchment area would be in close agreement with our and other larger-scale estimates (Table 3).

In more detailed studies at smaller scales and for individual catchments, aquatic C export was exclusively related to net ecosystem exchange (NEE) measured by eddy covariance. Here the estimated fractions of aquatic export range between 2 % of NEE in a temperate forest catchment (only discharge, evasion not considered, (Shibata et al., 2005)) and 160 % of NEE in a boreal peatland catchment (Billett et al., 2004). Analysis of inter-annual variations of stream export from a small peatland catchment in Sweden (Leach et al., 2016) resulted in estimates of C export by the fluvial network between 5.9 and 18.1 g Cm^{-2} yr^{-1} over 12 years. The total mean value of 12.2 g Cm^{-2} yr^{-1}, however, is in close agreement with the present and other larger-scale estimates (Table 3). In contrast to the present study, C export from the peatland catchments were dominated by stream discharge of dissolved organic carbon.

4.4 Controlling factors for aquatic C export

We found a significant linear relationship between total catchment NPP and the C export from the catchment in the stream network across four Strahler orders. The relationship was mainly caused by a strong correlation between catchment size and water surface area. As expected for temperate zones, large streams and rivers with large surface area have larger catchments. A study analyzing aquatic carbon fluxes for 18 hydrological units in the conterminous U.S. (Butman et al., 2015) observed a significant correlation between catchment-specific aquatic C yield and specific catchment NEP, which in turn was linearly correlated to NPP. We did not observe such correlation at smaller scale, which could be related to the rather narrow range of variability in NPP among the considered catchments. Nevertheless, the linear correlation observed by (Butman et al., 2015) indicates that a constant fraction of terrestrial NPP is exported by aquatic systems if averaged over larger spatial scales.

The relatively narrow range of variability of C export per catchment area (between 9 and 18 g C m^{-2} yr^{-1}, with the two exceptions discussed above) in different landscapes (Table 3) is rather surprising. Although this range of variation is most likely within the uncertainty of the various estimates, the variability across different landscapes is

certainly small in comparison to the order of magnitude differences in potential controlling factors like catchment NPP, fractional water coverage as well as size and climatic zone of the study area. In lake-rich regions, evasion from inland waters was observed to be dominated by lakes (Buffam et al., 2011;Jonsson et al., 2007), which cover up to 13 % of the surface area of these regions. In the present as well as in other studies on catchments where lakes are virtually absent (Wallin et al., 2013) and the fractional water coverage was smaller than 0.5 % of the terrestrial surface area, an almost identical catchment-specific C export and evasion rate has been observed (Table 3). CO_2 emissions from water surfaces depend on the partial pressure of CO_2 in water and are therefore related to DIC, which was the dominant form of dissolved C in the present study. Studies in the boreal zone, where dissolved C in the aquatic systems is mainly in the form of DOC, however, found comparable catchment-specific C export and evasion rates ((Leach et al., 2016;Jonsson et al., 2007;Wallin et al., 2013), cf. Table 3). The difference in the speciation of the exported C indicates that a larger fraction of the terrestrial NPP is respired by heterotrophic respiration in soils and exported to the stream network as DIC in the present study, in contrast to export as DOC and predominantly aquatic respiration. Observations and modeling of terrestrial-aquatic C fluxes across the U.S. suggested a transition of the source of aquatic CO_2 from direct terrestrial input to aquatic CO_2 production by degradation of terrestrial organic carbon with increasing stream size (Hotchkiss et al., 2015). Such transition was not observed in the present study, where organic carbon made a small contribution to the fluvial carbon load across all investigated stream orders. In addition to soil respiration, mineral weathering also contributes to DIC in stream water. The relative importance of soil respiration and weathering varies depending on geology and the presence of wetlands in the area (Hotchkiss et al., 2015;Lauerwald et al., 2013;Jones et al., 2003). In the present study, 16 % of the catchment areas contained carbonate bedrock. The DIC concentration in the water increased with the proportion of carbonate containing bedrock in the catchment (R^2=0.33, p<0.001).

Despite the small number of observations in the meta-analysis, the narrow range of variability of C export per catchment area may indicate that neither water surface area nor the location of mineralization of terrestrial derived C (soil respiration and export of DIC versus export of DOC and mineralization in the aquatic environment), are important drivers for the total C export from catchments by inland waters at larger spatial scales. This rather unexpected finding deserves further attention, as it suggests that other, currently poorly explored, processes control the aquatic-terrestrial coupling and the role of inland waters in regional C cycling. Given the significant contribution of inland waters to regional and global scale greenhouse gas emissions, the mechanistic understanding of these processes is urgently required to assess their vulnerability to ongoing climatic and land use changes, as well to the extensive anthropogenic influences on freshwater ecosystems. Recent developments of process-based models, which are capable of resolving the boundless biogeochemical cycle in the terrestrial–aquatic continuum from catchment to continental scales (Nakayama, 2016), are certainly an important tool for these future studies.

5 Conclusion:

Our analysis of the carbon budget in a temperate stream network on regional scale revealed a relationship of aquatic carbon export and terrestrial NPP. On average 2.7 % of the terrestrial NPP were exported from the catchments by rivers and stream with CO_2 evasion and downstream transport contributing equally to the export. A comparison of our regional scale study with other studies from different scales and landscapes showed a relatively narrow range of variability of carbon export per catchment area. Future research is needed to understand the processes that control the aquatic-terrestrial coupling and the role of inland waters in regional carbon cycling.

Acknowledgments

This study was financially supported by the German Research Foundation (grant no. LO 1150/9-1). We thank Miriam Tenhaken for contributing to a preliminary analysis. All raw data for this paper is properly cited and referred to in the reference list. The processed data, which were used to generate the figures and tables, are available upon request through the corresponding author.

References

Abril, G., Martinez, J.-M., Artigas, L. F., Moreira-Turcq, P., Benedetti, M. F., Vidal, L., Meziane, T., Kim, J.-H., Bernardes, M. C., Savoye, N., Deborde, J., Souza, E. L., Alberic, P., Landim de Souza, M. F., and Roland, F.: Amazon River carbon dioxide outgassing fuelled by wetlands, Nature, 505, 395-398, 10.1038/nature12797, 2013.

Abril, G., Bouillon, S., Darchambeau, F., Teodoru, C. R., Marwick, T. R., Tamooh, F., Omengo, F. O., Geeraert, N., Deirmendjian, L., and Polsenaere, P.: Technical Note: Large overestimation of pCO2 calculated from pH and alkalinity in acidic, organic-rich freshwaters, Biogeosciences, 12, 67, 2015.

Aufdenkampe, A. K., Mayorga, E., Raymond, P. A., Melack, J. M., Doney, S. C., Alin, S. R., Aalto, R. E., and Yoo, K.: Riverine coupling of biogeochemical cycles between land, oceans, and atmosphere, Front. Ecol. Environ., 9, 53-60, 10.1890/100014, 2011.

Barros, N., Cole, J. J., Tranvik, L. J., Prairie, Y. T., Bastviken, D., Huszar, V. L. M., del Giorgio, P., and Roland, F.: Carbon emission from hydroelectric reservoirs linked to reservoir age and latitude, Nature Geosci., 4, 593-596, 10.1038/ngeo1211, 2011.

Battin, T. J., Luyssaert, S., Kaplan, L. A., Aufdenkampe, A. K., Richter, A., and Tranvik, L. J.: The boundless carbon cycle, Nature Geosci., 2, 598-600, 10.1038/ngeo618, 2009.

Billett, M. F., Palmer, S. M., Hope, D., Deacon, C., Storeton-West, R., Hargreaves, K. J., Flechard, C., and Fowler, D.: Linking land-atmosphere-stream carbon fluxes in a lowland peatland system, Global Biogeochem. Cycles, 18, 10.1029/2003GB002058, 2004.

Buffam, I., Turner, M. G., Desai, A. R., Hanson, P. C., Rusak, J. A., Lottig, N. R., Stanley, E. H., and Carpenter, S. R.: Integrating aquatic and terrestrial components to construct a complete carbon budget for a north temperate lake district, Global Change Biol., 17, 1193-1211, 10.1111/j.1365-2486.2010.02313.x, 2011.

Butman, D., and Raymond, P. A.: Significant efflux of carbon dioxide from streams and rivers in the United States, Nature Geosci., 4, 839-842, 2011.

Butman, D., Stackpoole, S., Stets, E., McDonald, C. P., Clow, D. W., and Striegl, R. G.: Aquatic carbon cycling in the conterminous United States and implications for terrestrial carbon accounting, Proceedings of the National Academy of Sciences, 10.1073/pnas.1512651112, 2015.

Christensen, T. R., Johansson, T., Olsrud, M., Ström, L., Lindroth, A., Mastepanov, M., Malmer, N., Friborg, T., Crill, P., and Callaghan, T. V.: A catchment-scale carbon and greenhouse gas budget of a subarctic landscape, Philosophical Transactions of the Royal Society of London A: Mathematical, Physical and Engineering Sciences, 365, 1643-1656, 10.1098/rsta.2007.2035, 2007.

Cole, J. J., Prairie, Y. T., Caraco, N. F., McDowell, W. H., Tranvik, L. J., Striegl, R. G., Duarte, C. M., Kortelainen, P., Downing, J. A., Middelburg, J. J., and Melack, J.: Plumbing the global carbon cycle: Integrating inland waters into the terrestrial carbon budget, Ecosystems, 10, 171-184, 10.1007/s10021-006-9013-8, 2007.

DIN EN ISO 9963-1:1996-02: Wasserbeschaffenheit - Bestimmung der Alkalinität - Teil 1: Bestimmung der gesamten und der zusammengesetzten Alkalinität (ISO 9963-1:1994); German version EN ISO 9963-1:1995,

DIN EN ISO 9963-2:1996-02: Wasserbeschaffenheit - Bestimmung der Alkalinität - Teil 2: Bestimmung der Carbonatalkalinität (ISO 9963-2:1994); German version EN ISO 9963-2:1995,

DIN EN ISO 10523:2012-04: Wasserbeschaffenheit - Bestimmung des pH-Werts (ISO 10523:2008); German version EN ISO 10523:2012.

EEA: Corine Land Cover 2006 seamless vector data, European Environment Agency, 2006.

Hotchkiss, E. R., Hall Jr, R. O., Sponseller, R. A., Butman, D., Klaminder, J., Laudon, H., Rosvall, M., and Karlsson, J.: Sources of and processes controlling CO_2 emissions change with the size of streams and rivers, Nature Geosci., 8, 696-699, 10.1038/ngeo2507, 2015.

Jones, J. B., Stanley, E. H., and Mulholland, P. J.: Long-term decline in carbon dioxide supersaturation in rivers across the contiguous United States, Geophysical Research Letters, 30, 2003.

Jonsson, A., Algesten, G., Bergström, A. K., Bishop, K., Sobek, S., Tranvik, L. J., and Jansson, M.: Integrating aquatic carbon fluxes in a boreal catchment carbon budget, J. Hydrol., 334, 141-150, 10.1016/j.jhydrol.2006.10.003, 2007.

Lauerwald, R., Hartmann, J., Moosdorf, N., Kempe, S., and Raymond, P. A.: What controls the spatial patterns of the riverine carbonate system?—A case study for North America, Chemical geology, 337, 114-127, 2013.

Lauerwald, R., Laruelle, G. G., Hartmann, J., Ciais, P., and Regnier, P. A.: Spatial patterns in CO2 evasion from the global river network, Global Biogeochemical Cycles, 29, 534-554, 2015.

Leach, J. A., Larsson, A., Wallin, M. B., Nilsson, M. B., and Laudon, H.: Twelve year interannual and seasonal variability of stream carbon export from a boreal peatland catchment, J. Geophys. Res.-Biogeo., 121, 1851–1866, 10.1002/2016JG003357, 2016.

Leopold, L. B., and Maddock Jr, T.: The hydraulic geometry of stream channels and some physiographic implications2330-7102, 1953.

LVermGeoRP: Vermessungs- und Katasterverwaltung Rheinland-Pfalz, Landesamt für Vermessung und Geobasisinformation Rheinland-Pfalz, 2012.

Maberly, S. C., Barker, P. A., Stott, A. W., and De Ville, M. M.: Catchment productivity controls CO_2 emissions from lakes, Nat. Clim. Chang., 3, 391-394, 10.1038/nclimate1748, 2013.

MULEWF: GeoPortal Wasser, Ministerium für Umwelt, Landwirtschaft, Ernährung, Weinbau und Forsten Rheinland-Pfalz, 2013.

MULEWF: Wasserwirtschaftsverwaltung Rheinland-Pfalz, Ministerium für Umwelt, Landwirtschaft, Ernährung, Weinbau und Forsten Rheinland-Pfalz, 2015.

Nakayama, T.: New perspective for eco-hydrology model to constrain missing role of inland waters on boundless biogeochemical cycle in terrestrial–aquatic continuum, Ecohydrology & Hydrobiology, 16, 138-148, 10.1016/j.ecohyd.2016.07.002, 2016.

Parkhurst, D. L., and Appelo, C.: User's guide to PHREEQC (Version 2): A computer program for speciation, batch-reaction, one-dimensional transport, and inverse geochemical calculations, 1999.

R Development Core Team: R: A language and environment for statistical computing. R Foundation for Statistical Computing, Vienna, Austria, 2011.

Ran, L., Lu, X. X., Yang, H., Li, L., Yu, R., Sun, H., and Han, J.: CO_2 outgassing from the Yellow River network and its implications for riverine carbon cycle, J. Geophys. Res.-Biogeo., 120, 1334-1347, 10.1002/2015JG002982, 2015.

Randerson, J. T., Chapin, F. S., Harden, J. W., Neff, J. C., and Harmon, M. E.: Net ecosystem production: a comprehensive measure of net carbon accumulation by ecosystems, Ecol. Applications, 12, 937-947, 10.1890/1051-0761(2002)012[0937:NEPACM]2.0.CO;2, 2002.

Raymond, P. A., Oh, N.-H., Turner, R. E., and Broussard, W.: Anthropogenically enhanced fluxes of water and carbon from the Mississippi River, Nature, 451, 449-452, 2008.
Raymond, P. A., Zappa, C. J., Butman, D., Bott, T. L., Potter, J., Mulholland, P., Laursen, A. E., McDowell, W. H., and Newbold, D.: Scaling the gas transfer velocity and hydraulic geometry in streams and small rivers, Limnology and Oceanography: Fluids and Environments, 2, 41-53, 2012.
Raymond, P. A., Hartmann, J., Lauerwald, R., Sobek, S., McDonald, C., Hoover, M., Butman, D., Striegl, R., Mayorga, E., Humborg, C., Kortelainen, P., Durr, H., Meybeck, M., Ciais, P., and Guth, P.: Global carbon dioxide emissions from inland waters, Nature, 503, 355-359, 10.1038/nature12760, 2013.
Richey, J. E., Melack, J. M., Aufdenkampe, A. K., Ballester, V. M., and Hess, L. L.: Outgassing from Amazonian rivers and wetlands as a large tropical source of atmospheric CO_2, Nature, 416, 617-620, 10.1038/416617a, 2002.
Running, S. W., Nemani, R. R., Heinsch, F. A., Zhao, M., Reeves, M., and Hashimoto, H.: A Continuous Satellite-Derived Measure of Global Terrestrial Primary Production, Bioscience, 54, 547-560, 10.1641/0006-3568(2004)054[0547:acsmog]2.0.co;2, 2004.
Sabine, C. L., Heimann, M., Artaxo, P., Bakker, D. C., Chen, C.-T. A., Field, C. B., Gruber, N., Le Quéré, C., Prinn, R. G., and Richey, J. E.: Current status and past trends of the global carbon cycle, in: The Global Carbon Cycle, 2nd ed., edited by: Field, C. B., and Raupach, M. R., Scientific Committee on Problems of the Environment (SCOPE) Series, Island Press, 17-44, 2004.
Shibata, H., Hiura, T., Tanaka, Y., Takagi, K., and Koike, T.: Carbon cycling and budget in a forested basin of southwestern Hokkaido, northern Japan, Ecological Research, 20, 325-331, 10.1007/s11284-005-0048-7, 2005.
Stanley, E. H., Casson, N. J., Christel, S. T., Crawford, J. T., Loken, L. C., and Oliver, S. K.: The ecology of methane in streams and rivers: patterns, controls, and global significance, Ecological Monographs, 2016.
Statistisches Landesamt Rheinland-Pfalz: Statistisches Jahrbuch 2014, 2014.
Strahler, A. N.: Quantitative analysis of watershed geomorphology, Eos, Transactions American Geophysical Union, 38, 913-920, 1957.
Stumm, W., and Morgan, J. J.: Aquatic chemistry: chemical equilibria and rates in natural waters, Wiley, 1996.
Tranvik, L. J., Downing, J. A., Cotner, J. B., Loiselle, S. A., Striegl, R. G., Ballatore, T. J., Dillon, P., Finlay, K., Fortino, K., Knoll, L. B., Kortelainen, P. L., Kutser, T., Larsen, S., Laurion, I., Leech, D. M., McCallister, S. L., McKnight, D. M., Melack, J. M., Overholt, E., Porter, J. A., Prairie, Y., Renwick, W. H., Roland, F., Sherman, B. S., Schindler, D. W., Sobek, S., Tremblay, A., Vanni, M. J., Verschoor, A. M., von Wachenfeldt, E., and Weyhenmeyer, G. A.: Lakes and reservoirs as regulators of carbon cycling and climate, Limnol. Oceanogr., 54, 2298-2314, 10.4319/lo.2009.54.6_part_2.2298, 2009.
Wallin, M. B., Grabs, T., Buffam, I., Laudon, H., Ågren, A., Öquist, M. G., and Bishop, K.: Evasion of CO_2 from streams – The dominant component of the carbon export through the aquatic conduit in a boreal landscape, Global Change Biol., 19, 785-797, 10.1111/gcb.12083, 2013.

Walvoord, M. A., and Striegl, R. G.: Increased groundwater to stream discharge from permafrost thawing in the Yukon River basin: Potential impacts on lateral export of carbon and nitrogen, Geophysical Research Letters, 34, 2007.
Zhang, W., and Montgomery, D. R.: Digital elevation model grid size, landscape representation, and hydrologic simulations, Water Resour. Res., 30, 1019-1028, 10.1029/93WR03553, 1994.
Zhao, M., Heinsch, F. A., Nemani, R. R., and Running, S. W.: Improvements of the MODIS terrestrial gross and net primary production global data set, Remote Sensing of Environment, 95, 164-176, 10.1016/j.rse.2004.12.011, 2005.

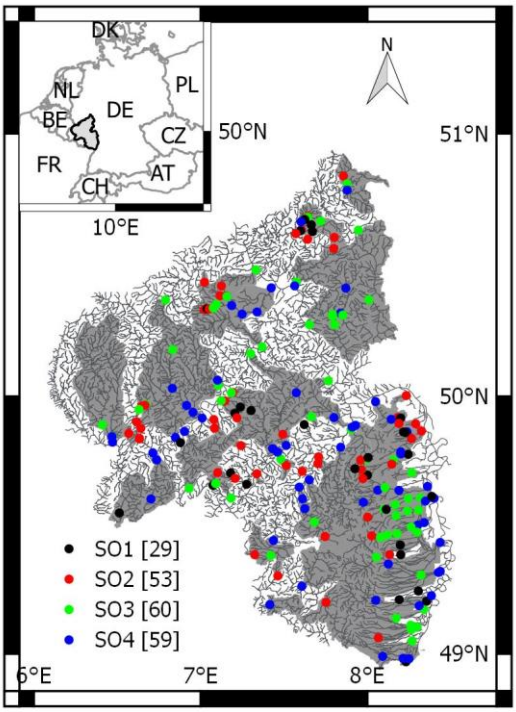

Fig. 1: Map of the stream network (black lines) within the state borders of Rhineland Palatinate in southwest Germany. The inset map in the upper left corner indicates the location of the study region in central Europe. Filled circles mark the position of sampling sites with color indicating stream order (SO1 – SO4; the numbers in brackets in the legend are the respective number of sampling sites). The catchment areas of the sampling sites are marked in grey color.

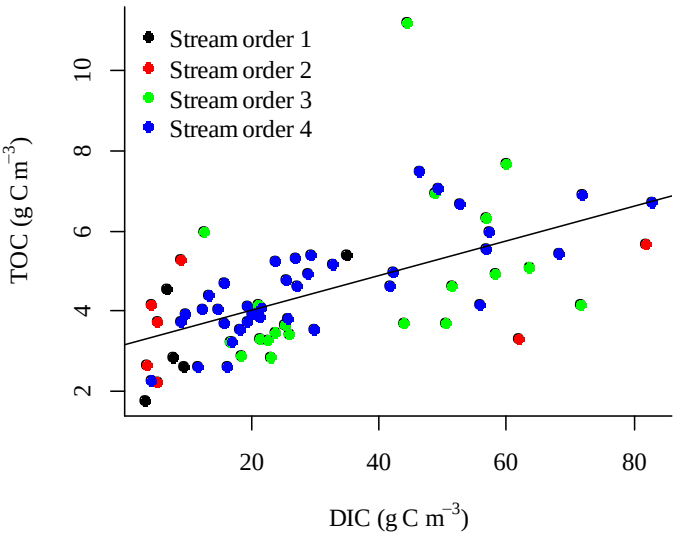

490

491 **Fig. 2: TOC concentration versus DIC concentration. Different colors indicate sampling sites from different stream**
492 **orders. The solid line shows the fitted linear regression model with TOC=0.04·DIC (r^2=0.33, p<0.001).**

493

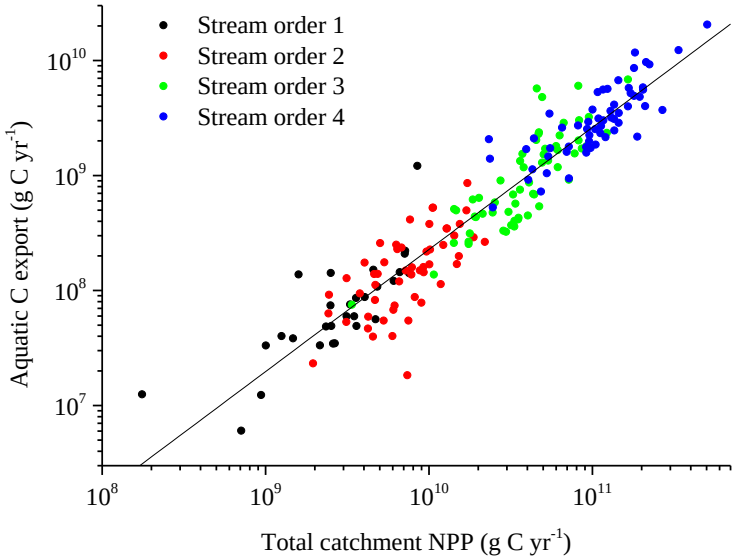

494

495 **Fig. 3: Annual rate of C export through the stream network versus terrestrial NPP in the catchment area. Different colors**
496 **indicate sampling sites from different stream orders. The solid line shows the fitted linear regression model for the log-**
497 **transformed data with C_export=0.005·NPP$^{1.06}$ (r^2=0.89, p<0.001).**

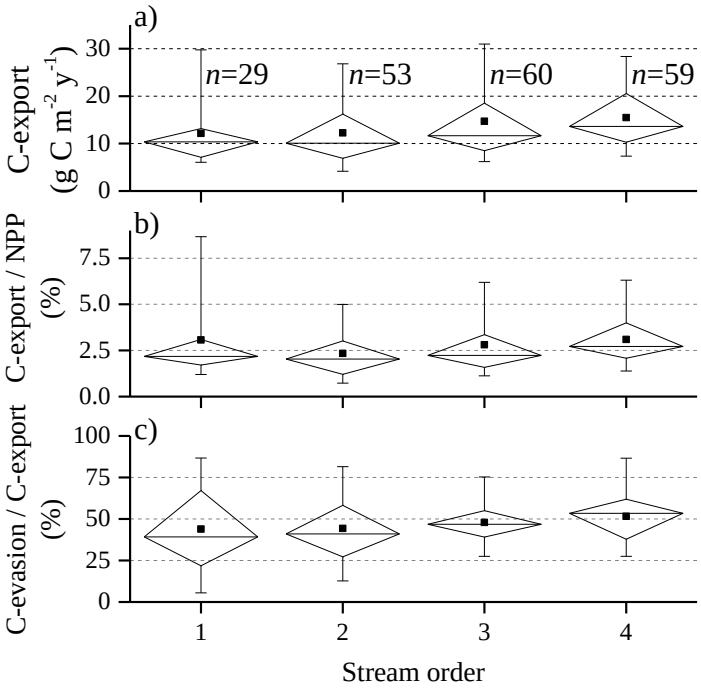

Fig. 4: a) Boxplots of C export (sum of evasion and discharge) normalized by catchment area. b) Boxplots of the ratio of the total exported C and terrestrial NPP for different stream orders. c) Boxplots of the fraction of the total exported C which is emitted to the atmosphere from the stream network for each stream order. The boxes demarcate the 25th and 75th percentiles, the whiskers demarcate the 95% confidence intervals. Median and mean values are marked as horizontal lines and square symbols, respectively. The sample numbers (*n*) provided in a) apply to all panels.

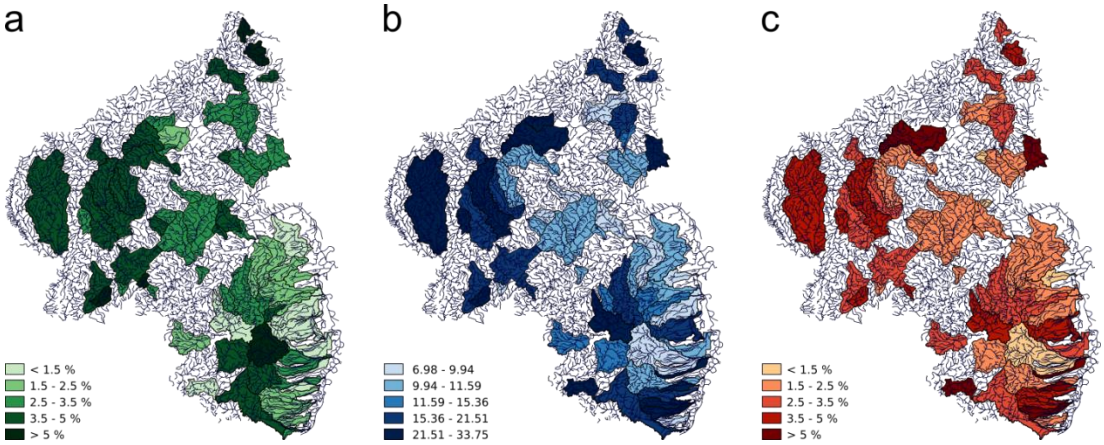

Fig. 5: Map of 3rd and 4th order catchments showing a) Mean NPP (g C m^{-2} yr^{-1}), b) aquatic export (g C m^{-2} yr^{-1}), c) ratio aquatic export/NPP (%).

509

510 **Table 1: Major hydrological characteristics, pCO_2, DIC and DOC concentrations averaged over stream orders (SO) and**
511 **for all sampling sites (total). All values are provided as mean±sd (standard deviation) of the annual mean observations,**
512 **ranges are given in brackets, *n* is the number of observations.**

	SO 1	**SO 2**	**SO 3**	**SO 4**	**Total**
n	29	53	60	59	201
Catchment size (km^2)	9±7 (1 – 35)	16±9 (4 – 37)	87±54 (9 – 298)	243±140 (48 – 889)	103±126 (1 – 889)
Water coverage (%)	0.24±0.11 (0.05 – 0.43)	0.26±0.09 (0.1 – 0.45)	0.36±0.11 (0.09 – 0.6)	0.42±0.13 (0.18 – 0.7)	0.33±0.13 (0.05 – 0.7)
Discharge ($m^3\ s^{-1}$)	0.06±0.05 (0.003 – 0.19)	0.15±0.10 (0.01 – 0.36)	0.73±0.63 (0.02 – 3.41)	2.20±1.95 (0.22 – 12.22)	0.91±1.41 (0.003 – 12.22)
Drainage rate ($m\ y^{-1}$)	0.26±0.17 (0.05 – 0.67)	0.29±0.16 (0.06 – 0.66)	0.27±0.17 (0.05 – 0.74)	0.30±0.21 (0.06 – 1.20)	0.28±0.18 (0.05 – 1.20)
pH	7.58±0.61 (6.20 – 8.97)	7.70±0.46 (6.30 – 8.60)	7.81±0.37 (6.60 – 8.30)	7.75±0.29 (6.91 – 8.30)	7.73±0.42 (6.20 – 8.97)
Alkalinity ($mmol\ L^{-1}$)	3.08±2.50 (0.08 – 7.58)	2.74±2.58 (0.08 – 8.55)	2.77±1.85 (0.14 – 9.88)	2.58±1.73 (0.32 – 7.22)	2.75±2.12 (0.08 – 9.88)
pCO_2 (ppm)	2597±1496 (145 – 6706)	1819±1095 (681 – 5338)	1992±1327 (573 – 7627)	2162±1302 (366 – 7759)	2083±1303 (145 – 7759)
DIC ($g\ m^{-3}$)	38.8±30.3 (3.4 – 93.1)	34.2±31.1 (3.5 – 104.5)	34.6±22.4 (3.1 – 119.6)	32.4±21.0 (4.1 – 89.3)	34.5±25.7 (3.1 – 119.6)
DOC ($g\ m^{-3}$)	3.54±1.86 (2.2 – 6.7) (*n*=5)	4.11±0.73 (3.1 – 4.8) (*n*=4)	4.17±1.08 (2.6 – 7.1) (*n*=22)	4.10±1.24 (2.0 – 7.7) (*n*=33)	4.08±1.20 (2.0 – 7.7) (*n*=64)

513

514 **Table 2: Aquatic C-fluxes and terrestrial NPP in catchments drained by streams of different stream orders (SO) and for**
515 **all sampling sites (total). All values are mean ± standard deviation, ranges are given in brackets. The CO_2 flux from the**
516 **water surface (first row) is expressed per square meter water surface area, while the remaining fluxes are expressed per**
517 **square meter catchment area.**

	SO 1	SO 2	SO 3	SO 4	Total
CO_2 flux from water surface ($g\ C\ m^{-2}\ yr^{-1}$)	2415±2335 (-335 – 12915)	1975±1364 (418 – 7143)	1998±1671 (704 – 11016)	1928±903 (851 – 5093)	2032±1528 (-335 – 12915)
Gas transfer velocity k600 ($m\ d^{-1}$)	7.04±4.52 (2.16 – 20.57)	7.74±3.78 (2.03 – 20.50)	5.86±2.81 (2.03 – 15.55)	4.23±0.96 (2.03 – 6.50)	6.05±3.32 (2.03 – 20.57)
CO_2 evasion per catchment area ($g\ C\ m^{-2}\ yr^{-1}$)	5.9±6.3 (-1.0 – 30.0)	5.2±4.1 (0.7 – 19.2)	7.0±6.6 (1.6 – 43.8)	8.0±4.6 (3.0 – 23.0)	6.6±5.5 (-1.0 – 43.8)
DIC discharge per catchment area ($g\ C\ m^{-2}\ yr^{-1}$)	6.2±4.5 (1.6 – 25.8)	7.1±6.1 (0.6 – 27.2)	7.7±5.7 (1.6 – 35.5)	7.5±4.7 (1.2 – 24.5)	7.3±5.4 (0.6 – 35.5)
Total aquatic C export per catchment area ($g\ C\ m^{-2}\ yr^{-1}$)	12.1±6.9 (4.7 – 34.5)	12.3±6.9 (1.5 – 29.6)	14.7±10.8 (5.3 – 66.8)	15.5±6.7 (7.0 – 33.8)	13.9±8.3 (1.5 – 66.8)
NPP ($g\ C\ m^{-2}\ yr^{-1}$)	466±127 (106 – 661)	536±66 (251 – 644)	527±57 (364 – 627)	508±69 (330 – 618)	515±79 (106 – 661)

Table 3: Summary of estimates of aquatic C export in relation to terrestrial production in the watershed across different spatial scales (spatial scale decreases from top to bottom). Aquatic C export is the sum of C-discharge and evasion (numbers in parentheses also include the change in C storage in the aquatic systems by sedimentation) normalized by the area of the terrestrial watershed. Aquatic C fate refers to the percentage of the total exported C which is emitted to the atmosphere (evasion) and transported downstream (discharge). The missing percentage is the fraction which is stored in the aquatic systems by sedimentation (if considered). Terrestrial production is expressed as NPP or as net ecosystem exchange (NEE). n.c. indicates that this compartment/flux was not considered in the respective study.

Study area (Catchment size in km^2)	Fractional water coverage (%) Rivers Lakes	Aquatic C export ($g\ C\ m^{-2}\ yr^{-1}$)	Aquatic C fate (%): Evasion Discharge	Aquatic C export / terrestrial production (%)		Reference
				NPP	NEE	
Global ($1.3x10^8$)	R: 0.2-0.3 L: 2.1-3.4	16 (20)	E: 44 D: 34	3.7 [1]	21-64 [2]	(Aufdenkampe et al., 2011)
Conterminous U.S. ($7.8x10^6$)	R: 0.52 L: 1.6	13.5 (18.8)	E: 58 D: 28	3.6	27 [3]	(Butman et al., 2015)
Central Amazon ($1.8x10^6$)	4-16	78	E: 87 D: 13	6.8 [4]	n.c.	(Richey et al., 2002)
Yellow River network ($7.5x10^5$)	R: 0.3-0.4 L: n.c.	18.5 (30)	E: 35 D: 26	n.c.	96 (62)	(Ran et al., 2015)
North temperate	R: 0.5	11.8	E: 33	n.c.	7	(Buffam et al.,

lake district (6400)	L: 13	(16)	D: 41			2011)
Northern Sweden (peat) (3025)	R: 0.33 L: 3.5	9	E: 50 (4.5) D: 50 (4.5)	n.c.	6	(Jonsson et al., 2007)
Temperate streams (0.7- 1227)	**R: 0.33** **L: n.c.**	**13.9**	E: 47 D: 53	**2.7**	n.c.	**This study**
English Lake district (1 - 360)	R: n.c. L: 2.2	5.4	E: 100 D: n.c.	1.6	n.c.	(Maberly et al., 2013)
Forested stream catchments in Sweden (0.46 - 67)	R: 0.1-0.7 L:n.c. (<0.7)	9.4	E: 53 D: 47	n.c.	8-17	(Wallin et al., 2013)
Forest catchment in Japan (9.4)	R: - L: n.c.	4	E: n.c. D: 100	n.c.	2	(Shibata et al., 2005)
Peatland catchment (3.35)	R: 0.05 L: n.c.	30.4	E: 13 D: 87	n.c.	160	(Billett et al., 2004)
Peatland catchment (2.7)	R: n.c. L: 2.2	12.2	E: - D: -	n.c.	12-50	(Leach et al., 2016)

[1] For a value of 56 Pg C yr^{-1} for global NPP (Zhao et al., 2005).

[2] Global mean NEE was estimated as the difference of GPP and ecosystem respiration, which was assumed to be 91-97 % of GPP (Randerson et al., 2002).

[3] This percentage refers to NEP instead of NEE.

[4] For a global mean value of NPP in tropical forests of 1148 g C m^{-2} yr^{-1} (Sabine et al., 2004).